

Investigation of the Effects of Atmospheric Attenuation and Frequency on MIMO Channel Capacity

Ahmet Furkan Kola and Cetin Kurnaz


Abstract— The efficiencies of 5G channels, which are highly affected by atmospheric attenuation, are still being investigated. The effects of frequency and atmospheric attenuation parameters such as humidity, temperature, rain, and pressure were investigated in this study using the NYUSIM program. The spatial consistency mode of the NYUSIM channel simulator was turned off, and unnormalized channel capacities were calculated at 28, 45, 60, and 73 GHz frequencies. According to the research results, the rain rate was the atmospheric attenuation parameter that significantly affected MIMO channel capacity. In contrast, the humidity percentage had the slightest impact. The frequency where the channel capacity is most affected by the four determined atmospheric attenuation parameters is 60 GHz, while the frequency where it is least affected is 28 GHz. The study found that using frequencies with high atmospheric attenuation reduces communication efficiency significantly. Furthermore, rain rate has a significant impact on 5G channel performance.

Index Terms—Atmospheric attenuation, Channel capacity, Channel modeling, mmWave, NYUSIM


I. INTRODUCTION

THE INTERNATIONAL Telecommunication Union (ITU) attempted to meet the growing demand for data rate with the fifth-generation (5G) technology. New technologies such as IoT, cloud, and intelligent systems add new bits to mobile communication has limited the use of the existing frequency region. Using the millimeter wave (mmWave) region with 5G has been motivated. The extremely high frequency (EHF) region, planned for 5G and beyond systems, aims to reach frequencies of up to 300 GHz and achieve extremely high data rates.

AHMET FURKAN KOLA, is with Department of Electrical and Electronics Engineering, Samsun University, Samsun, Turkey, (e-mail: ahmet.kola@samsun.edu.tr).

 <https://orcid.org/0000-0003-0510-3255>

CETIN KURNAZ, is with Department of Electrical and Electronics Engineering, Ondokuz Mayıs University, Samsun, Turkey, (e-mail: ckurnaz@omu.edu.tr).

 <https://orcid.org/0000-0003-3436-899X>

Manuscript received Oct 25, 2022; accepted July 31, 2023.

DOI: [10.17694/bajece.1210093](https://doi.org/10.17694/bajece.1210093)

The communication system in mmWave technologies has been determined as Multiple-Input Multiple-Output (MIMO) Orthogonal Frequency-Division Multiplexing (OFDM). Existing MIMO systems have been converted to massive MIMO (m-MIMO) techniques to increase channel capacity and data rate by increasing the number of antennas. This technology can be developed due to the antenna sizes, which decrease inversely correspondingly to frequency increase. The OFDM technique, also used in existing communication systems, has been maintained by increasing the bandwidth to 800 MHz. Thus, the disruptive effect of the channel is eliminated by dividing the fast-fading channels into fixed-fading sub-channels [1].

Signal powers decreased as the frequency of mmWave communication increased, as did antenna lengths and communication distances between antennas. Furthermore, atmospheric attenuation begins to have a more significant impact on the signals. Meteorological factors such as temperature, humidity, air dryness, pressure, vapor, rain, and haze all affect the quality of mmWave communication. These innovations and disruptive effects necessitated the development of new mobile communication channel models. Many simulation programs are available to demonstrate how these models can be generated and how disruptions affect the models. WinProb [2] and QuaDRiGa [3], which create deterministic models, as well as MiliCar [4] and NYUSIM [5], which generate stochastic models, are among them. In this study, the NYUSIM channel simulator designed by Sun, MacCartney, and Rappaport in 2017 was used. Many studies have explored the power delay profile (PDP) and path loss models generated by the NYUSIM channel simulator [6-8]. There are also studies using this simulator to investigate the effects of meteorological variables on the channel [9-13] and the results of some of these parameters on channel capacity [14-16]. Aside from this simulator, the effects of meteorological variables on 5G systems have been studied [17,18]. Related researchs have demonstrated that mmwaves are significantly impacted by atmospheric processes, particularly as rain increases and absorption and scattering become more pronounced. However, the impact of all these variables on channel capacity has not been studied in detail.

This study investigated the effects of temperature, humidity, barometric pressure, and rain rate parameters on MIMO channel capacity at different frequencies using the NYUSIM

channel simulator. In this way, it has been determined which meteorological conditions affect the channels the most and what precautions should be taken. The responses of various high frequencies to these parameters were also investigated and evaluated.

II. MILLIMETER WAVE COMMUNICATION

The extreme congestion of the sub-6 GHz bands has encouraged different frequency bands in mobile communication. With its unlicensed use and wide bandwidths, mmWave transmission, the ITU's standards will be appropriate for the developing technology. MDue to the smaller antenna sizes in mmWave communication, more antennas can be placed at base stations. This way, the number of MIMO antennas for each communication can increase. Increasing the number of antennas to 64, 128, and 256 is called massive MIMO. The number of antennas per user decreases as the number of antennas increases. Furthermore, to communicate, these antennas, which increase in number with increasing frequency and declining signal strength, must be placed close to each other. Although costly, this system will reduce the intersymbol interference (ISI) and minimize the attenuation effects such as propagation and fading. The distortion effect of the channel increases with both the increase in carrier frequency and the increase in bandwidth in mmWave communication. To resolve this, the OFDM technique, which began with 4G, expanded to 5G. The deep fading points of the channel increase in agreement with the increase in bandwidth. The OFDM technique attempts to fix this problem by dividing the channel into sub-channels. It makes the fast fading channel locally flat faded and transmits with these sub-channels by dividing it into N sub-channels. In this way, it simplifies communication and avoids the channel's disruptive effects [1].

III. CHANNEL MODELLING

A communication model consists of a receiver, transmitter, and channel. The signal transmitted from the transmitter $x(t)$ a signal at the receiver is $y(t)$. The impulse response of the channel is $h(t)$ and noise $n(t)$ and is expressed by Eq. (1). These variables all depend on time represented with t . Also, τ is a time variable.

$$y(t) = x(t) * h(t) + n(t) \tag{1}$$

$$= \int_{-\infty}^{\infty} h(\tau)x(t - \tau)d\tau + n(t)$$

If the communication has two inputs and two outputs, it is mathematically expressed as Eq. (2).

$$\begin{bmatrix} y_1 \\ y_2 \end{bmatrix} = \begin{bmatrix} h_{11} & h_{12} \\ h_{21} & h_{22} \end{bmatrix} \begin{bmatrix} x_1 \\ x_2 \end{bmatrix} + \begin{bmatrix} n_1 \\ n_2 \end{bmatrix} \tag{2}$$

For m inputs and n outputs, the channel is denoted by Eq. (3).

$$H_{m \times n} = \begin{bmatrix} h_{11} & h_{12} & \dots \\ h_{21} & h_{22} & \dots \\ \vdots & \vdots & h_{mn} \end{bmatrix} \tag{3}$$

The channel between the first antennas at the receiver and the transmitter is denoted by h_{11} . This value is obtained when the signal is reflected, refracted, or directly reaches the receiver during transmission. If the signal goes in a direct path, it is referred to as the line of sight (LOS); if it goes as a result of reflections, it is referred to as a non-line of sight (NLOS). h_{11} and all other MIMO channels can be represented by only one of these transmitted signals (flat fading) or by the shifted sum of these signals arriving one after the other at different times (fast fading) [19]. Additionally, the signal can reach the receiver by being attenuated by the channel and interfering with other communication channels. As a result of these disruptive effects, the signal fades before going to the receiver. The use of high frequencies with 5G revealed the disruptive effects of atmospheric attenuation. Fig. 1 depicts atmospheric sea-level attenuation in the 1-100 GHz dB frequency range. The regions marked in red in the figure show fading at the 28, 45, 60, and 73 GHz frequencies used in this study. Because 28 and 73 GHz have the lowest fading locally, 60 GHz has the highest fading in the determined range, and 45 GHz is just before the fading slope increases.

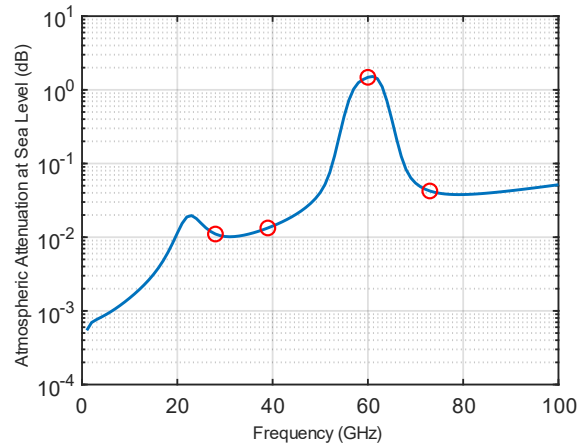


Fig.1. Atmospheric attenuation at sea level

A. NYUSIM Channel Model

In this study, the NYUSIM channel simulation V3.1 spatial consistency mode is turned off, and evaluations are performed for stationary users. Channel model measurements were taken for 28 and 73 GHz carrier frequencies. The channel model creates channel impulse responses (CIRs) using the concepts of time cluster (TC) and spatial lobe (SL). The simulator generates different stochastic channels at each run based on the parameters. Therefore, each scenario was created to repeat at least 2000 times and averaged during the analysis.

NYUSIM is a MATLAB program that calculates the frequency response of the channel. In the frequency (f) region, m is the number of transmitters, k is the receivers, and p is the components above -40 dB, which is considered stronger than noise, and all MIMO-OFDM subcarriers are represented in Eq. (4).

$$h_{mk}(f) = \sum_p \alpha_{m,k,p} e^{j\phi} e^{-j2\pi f\tau} e^{-j2\pi d_T m \sin(\theta)} e^{-j2\pi d_R k \sin(\varphi)} \tag{4}$$

Here, α is the amplitude of the antenna gain, Φ is the phase of each multipath component (MPC), τ is the delay of the MPC, d_T is the distance between MIMO transmitters, and d_R is the distance between each antenna at the receiver. θ and φ represent azimuth angles.

In NYUSIM, a close-in free space reference distance (CI) path loss model with a reference point of 1 m is used depending on various atmospheric attenuation factors. It is expressed by PL^{CI} and calculated by Eq. (5).

$$PL^{CI}(f, d) = FSPL(f, 1m) + 10n\log_{10}(d) + AT + X_{\sigma}^{CL} \quad (5)$$

Here, d is the distance between the transceiver, n is the path loss exponent (PLE) value, and X_{σ}^{CL} is a zero-mean Gaussian random variable with a standard deviation σ in dB named shadow fading. The free space path loss model (FSPL) in dB can be calculated with Eq. (6).

$$FSPL(f, 1m)[dB] = 20 \log_{10} \left(\frac{4\pi f \times 10^9}{c} \right) \quad (6)$$

Where f represents the carrier frequency in GHz, and c represents the speed of light. Atmospheric attenuation in dB can be calculated in terms of α attenuation coefficient and distance with Eq. (7).

$$AT[dB] = \alpha[dB/m] + d[m] \quad (7)$$

The coefficient α is expressed here as a function of dry air, haze, fog, rain, and vapor effect between 1 GHz and 100 GHz. Fig. 2 depicts the impact of these parameters individually, as shown by NYUSIM, on various frequencies [20].

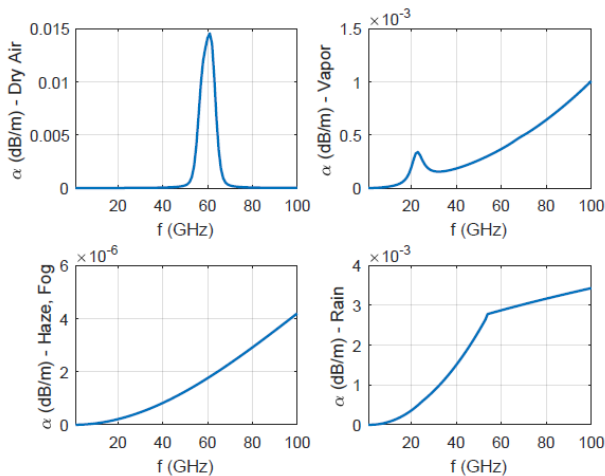


Fig.2. Propagation attenuation due to dry air, vapor, haze/fog, and rain at mmWave frequencies

B. Channel Capacity

This study made channel capacity calculations for the unnormalized channel condition. The measure of channel capacity can be expressed with Eq. (8) for MIMO channels.

$$C = B \log_2 [\det (I_m + SNR \cdot H \cdot H')] \quad (8)$$

Where H stands for the channel matrix, and H' stands for the conjugated transpose of the channel matrix. I_m represents the identity matrix with dimensions $m \times m$ and SNR means Signal-to-Noise ratio.

This study performed the capacity analysis in the frequency domain as given in Eq. (9).

$$C = B \sum_1^r \log_2 (1 + SNR \cdot \lambda_i^2) \quad (9)$$

Here, λ_i^2 represents the eigenvalues of the $H \cdot H'$ matrix.

IV. ANALYSIS RESULTS

The layers of Using the NYUSIM channel simulator, the effects of rain rate, barometric pressure, humidity, temperature, and frequency on MIMO channel capacity were investigated. The parameters used in the simulations are summarized in Table I. The Power Delay Profile (PDP) of the channel produced by the NYUSIM program, whose properties are determined by Table I (1013.25 mbar barometric pressure, 20 °C temperature, 80% humidity, 5 mm/hr rain rate), is shown in Fig. 3. PDP is made up of delayed reflections that arrive at the receiver at different strengths. The frequency response of this channel is shown in Fig. 4. The signal has an average power of -44.84 dBm and a bandwidth of 800 MHz around the carrier frequency of 28 GHz.

TABLE I
CHANNEL PARAMETERS

Channel Parameters	Scenarios			
	1	2	3	4
Frequencies	28, 45, 60, 73 GHz			
Environment	LOS			
Bandwidth	800 MHz			
MIMO	2 x 2			
Scenario	UMa			
Distance	100 m			
Tx Power	30 dBm			
Rain Rate	Variable	5 mm/hr	5 mm/hr	5 mm/hr
Barometric Pressure	1013.25 mbar	Variable	1013.25 mbar	1013.25 mbar
Humidity	80%	80%	Variable	80%
Temperature	20 °C	20 °C	20 °C	Variable

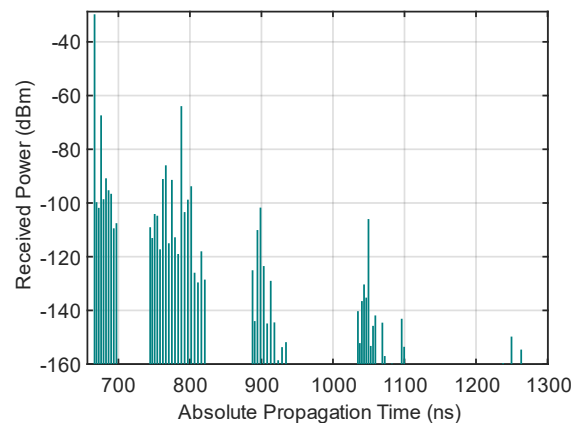


Fig.3. A sample of channel impulse response value in time-domain

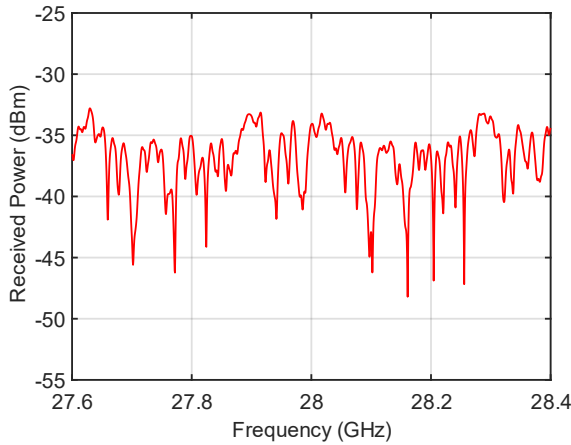


Fig.4. An example of OFDM subcarrier presentation in the frequency domain

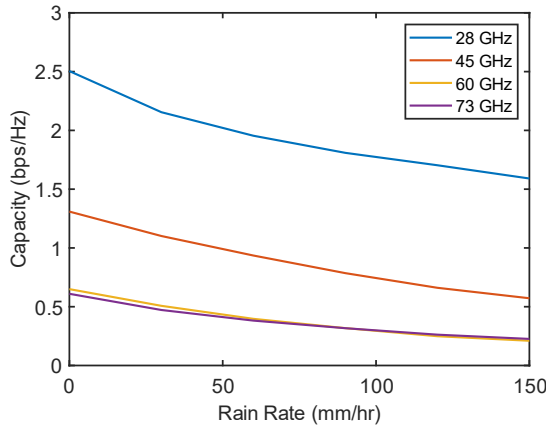


Fig.5. The effect of rain rate on channel capacity

A. Rain Rate Effect

All other parameters were held constant except for the rain rate, and the effect of this value on channel capacity was examined. Fig. 5 depicts the extent of the impact of the four different frequencies determined by the precipitation rate by channel capacity as a result of the analysis. The results were analyzed between conditions with no rain and a 150 mm rain rate per hour. When the simulation results are examined, the channel capacity at 28 GHz frequency is 2.5043 in the absence of rain and 1.5907 in the case of 150 mm/hr precipitation, representing a 36.48% decrease in channel capacity. When the 45 GHz frequency is examined, while the capacity is 1.3092 for 0 mm/hr, it is 0.5720 for 150 mm/hr, representing a 56.31% decrease in channel capacity. For 60 GHz, the capacity is 0.6497 in the absence of rain and 0.2104 in the case of the highest rain rate. The capacity was reduced by 67.62%. At 73 GHz, the capacity is 0.6099 for 0 mm/hr and 0.2260 for 150 mm/hr, representing a 62.94% reduction in channel capacity. The results showed that the frequency most affected by rain was 60 GHz. For 60 GHz frequency, 90 mm/hr, and above rain rate, the channel capacity is below the capacity of the 73 GHz channel. The frequency least affected by the rain rate as a percentage is 28 GHz.

B. Barometric Pressure Effect

The effect of Barometric Pressure on channel capacity was examined using the channel parameters shown in Table I. Fig. 6 depicts the decrease in the capacities of four different frequencies due to the analyses with increasing pressure. The results were examined between 100 mbar and 1013.25 mbar pressure values. As shown in Fig. 6, while the 60 GHz frequency is highly affected by pressure increases, such a decrease in capacity was not observed at other frequencies. The 28 GHz frequency capacity is 2.4837 for 100 mbar pressure, while it is 2.4696 for 1013.25 mbar, and there is a 0.56% decrease in channel capacity. When the frequency of 45 GHz is examined, while the capacity for 100 mbar is 1.2906, it is 1.2795 for 1013.25 mbar pressure. There is a 0.86% reduction in channel capacity. At 100 mbar pressure for 60 GHz, the capacity was 0.8011, while at 1013.25 mbar, it was 0.6243, representing a capacity decrease of 22.07%. At the 73 GHz frequency, while the capacity is 0.5963 for 100 mbar, it is 0.5752 for 1013.25 mbar, and there is a 3.54% reduction in channel capacity. The 60 GHz frequency experienced the most significant decrease in channel capacity as pressure increased. The least affected frequency is 28 GHz.

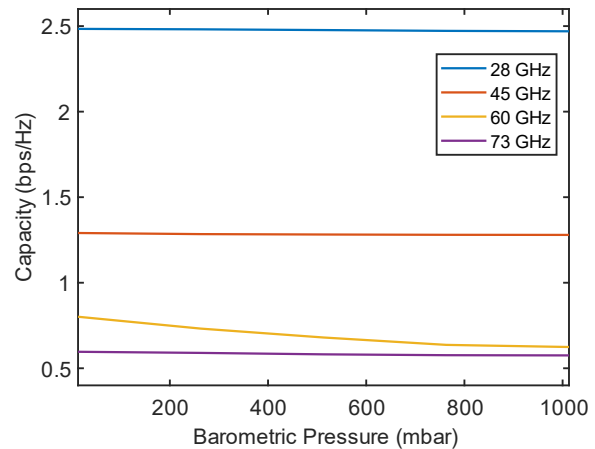


Fig.6. The effect of barometric pressure on channel capacity

C. Humidity Effect

The effect of humidity percentage on channel capacity was investigated for 28, 45, 60, and 73 GHz frequencies. Humidity was examined between 0% and 100%, and the results are shown in Fig. 7. When the simulation results are analyzed, the 28 GHz frequency has the highest channel capacity of 2.5006 in a 60% humidity environment and the lowest value of 2.4695 in a 100% humidity environment. Channel capacity was reduced by 1.24%. When the 45 GHz frequency is examined, while the capacity is 1.2912 for 0% humidity, it is 1.2542 for 100%, and there is a 2.86% decrease. For 60 GHz, the capacity is 0.5737 at 0 humidity, 0.6109 at 60% humidity, and a 6.09% change in capacity is seen. At the 73 GHz frequency, while the capacity is 0.5786 for 60% humidity, it is 0.5582 for 100% humidity, and there is a 3.52% reduction in channel capacity. As a result, the frequency most affected by humidity change is 60 GHz, while the least affected frequency is 28 GHz.

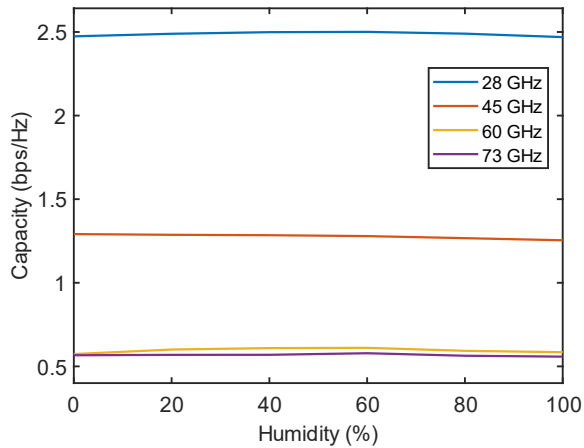


Fig.7. The effect of humidity percentage on channel capacity

D. Temperature Effect

The effect of temperature on the channel capacity was investigated between -10°C and 40°C , and the results are shown in Fig. 7. The 28 GHz frequency capacity has a minimum value of 2.4692 at 20°C , and the capacity has increased for increasing and decreasing values from this temperature. The highest capacity was obtained as 2.4934 for -10°C , and the variation in capacity was 0.97%. The lowest capacity value for the 45 GHz frequency is 20°C , while the highest capacity value is -10°C . Capacity values are 1.2804 and 1.2758, respectively, and there is a 0.35% reduction in channel capacity. For 60 GHz, the capacity at -10°C is calculated to be 0.5563, and the channel capacity increases with increasing temperature at this frequency. For 40°C temperature, the capacity is 0.6382, and an increase of 12.83% was seen. At the 73 GHz frequency, the capacity is highest at 10°C , while the channel capacity decreases with increasing and decreasing temperatures. For 10°C , the capacity is 0.5784, while for 40°C , it is 0.5555, and there is a 3.96% reduction in channel capacity. The temperature effect has the most significant effect on 60 GHz, while 45 GHz has a minor impact.

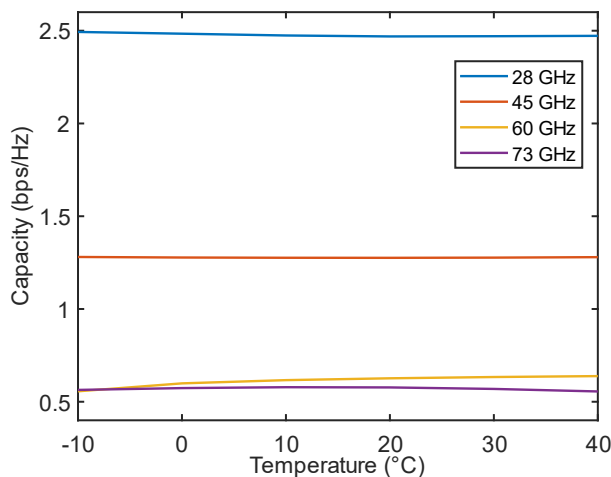


Fig.8. The effect of temperature on channel capacity

V. CONCLUSION

In this study, the effects of atmospheric attenuation parameters such as temperature, humidity percentage, rain rate, and barometric pressure on MIMO channel capacity were investigated using the NYUSIM channel simulator. In channel simulations, frequencies of 28, 45, 60, and 73 GHz were used. From the results of the analysis, it was seen that the 60 GHz frequency was the most affected by the four different parameters. 73 GHz is the second most affected frequency. While the frequency of 28 GHz was the least affected by the other three parameters except for temperature, it affected the frequency of 45 GHz at least by the temperature change. For the 60 GHz frequency, the rain rate had the most significant effect on channel capacity, with a variation of 67.62%, while humidity had the most negligible impact, with 6.09%. While a change in barometric pressure reduces capacity by 22.07%, a temperature change reduces capacity by 12.83%.

These results indicate that frequency selection is critical in next-generation mobile communication. It does not appear possible to achieve efficiency at frequencies with high atmospheric attenuation. Local minimum atmospheric attenuation (24-30 GHz/37-40 GHz/67-73 GHz) should be preferred when selecting a higher frequency. It is also understood that it will be more challenging to use at high frequencies with high attenuation, especially in heavy rain environments. In future studies, different channel parameters such as transceiver distance, different channel scenarios, different bandwidths will be evaluated, and analyses will be carried out with other comparisons such as path loss and received power. Apart from NYUSIM, it is also planned to compare different channel models with the simulator.

REFERENCES

- [1] Wang, X., Kong, L., Kong, F., Qiu, F., Xia, M., Arnon, S., & Chen, G. (2018). Millimeter-wave communication: A comprehensive survey. *IEEE Communications Surveys & Tutorials*, 20(3), 1616-1653.
- [2] WinProp, Wave Propagation and Radio Network Planning Software (part of Altair HyperWorks), www.altairhyperworks.com/WinProp.
- [3] Jaeckel, S., Raschkowski, L., Börner, K., & Thiele, L. (2014). QuaDRiGa: A 3-D multi-cell channel model with time evolution for enabling virtual field trials. *IEEE transactions on antennas and propagation*, 62(6), 3242-3256.
- [4] Drago, M., Zugno, T., Polese, M., Giordani, M., & Zorzi, M. (2020, June). MilliCar: An ns-3 module for mmWave NR V2X networks. In *Proceedings of the 2020 Workshop on ns-3* (pp. 9-16).
- [5] Samimi, M. K., & Rappaport, T. S. (2016). 3-D millimeter-wave statistical channel model for 5G wireless system design. *IEEE Transactions on Microwave Theory and Techniques*, 64(7), 2207-2225.
- [6] Lodro, M. M., Majeed, N., Khuwaja, A. A., Sodhro, A. H., & Greedy, S. (2018, March). Statistical channel modeling of 5G mmWave MIMO wireless communication. In *2018 International Conference on Computing, Mathematics and Engineering Technologies (iCoMET)* (pp. 1-5). IEEE.
- [7] Momo, S. H. A., & Mowla, M. M. (2019, July). Statistical analysis of an outdoor mmWave channel model at 73 GHz for 5G networks. In *2019 International Conference on Computer, Communication, Chemical, Materials and Electronic Engineering (IC4ME2)* (pp. 1-4). IEEE.
- [8] Zekri, A. B., Ajgou, R., Chems, A., & Ghendir, S. (2020, May). Analysis of Outdoor to Indoor Penetration Loss for mmWave Channels. In *2020 1st International Conference on Communications, Control Systems and Signal Processing (CCSSP)* (pp. 74-79). IEEE.
- [9] Alfaresi, B., Nawawi, Z., Malik, R. F., Anwar, K., & Nur, L. O. (2020). Humidity Effect to 5G Performances Under Palembang Channel Model At 28 GHz. *Sinergi*, 24(1), 49-56.

- [10] Budalal, A. A., Rafiqul, I. M., Habaebi, M. H., & Rahman, T. A. (2019). The effects of rain fade on millimeter-wave channel in tropical climate. *Bulletin of Electrical Engineering and Informatics*, 8(2), 653-664.
- [11] Rahman, M. N., Anwar, K., & Nur, L. O. (2019, November). Indonesia 5G channel model considering temperature effects at 28 GHz. In 2019 Symposium on Future Telecommunication Technologies (SOFTT) (Vol. 1, pp. 1-6). IEEE.
- [12] Dimce, S., Amjad, M. S., & Dressler, F. (2021, March). mmwave on the road: Investigating the weather impact on 60 GHz v2x communication channels. In 2021 16th Annual Conference on Wireless On-demand Network Systems and Services Conference (WONS) (pp. 1-8). IEEE.
- [13] Larasati, S., Yuliani, S. R., & Danisya, A. R. (2020). Outage Performances of 5G Channel Model Influenced by Barometric Pressure Effects in Yogyakarta. *Jurnal Infotel*, 12(1), 25-31.
- [14] Prasetyo, A. H., Suryanegara, M., & Asvial, M. (2019, December). Evaluation of 5G Performance at 26 GHz and 41 GHz frequencies: The Case of Tropical Suburban Areas in Indonesia. In 2019 IEEE 14th Malaysia International Conference on Communication (MICC) (pp. 101-105). IEEE.
- [15] Hikmaturokhman, A., Suryanegara, M., & Ramli, K. (2019, June). A comparative analysis of 5G channel model with varied frequency: a case study in Jakarta. In 2019 7th International Conference on Smart Computing & Communications (ICSCC) (pp. 1-5). IEEE.
- [16] Kurniawan, A., Danisya, A. R., & Isnawati, A. F. (2020, December). Performance of mmWave Channel Model on 28 GHz Frequency Based on Temperature Effect in Wonosobo City. In 2020 IEEE International Conference on Communication, Networks, and Satellite (Comnetsat) (pp. 37-41). IEEE.
- [17] Kourogorgas, C., Sagkriotis, S., & Panagopoulos, A. D. (2015, April). Coverage and outage capacity evaluation in 5G millimeter wave cellular systems: impact of rain attenuation. In 2015 9th European Conference on Antennas and Propagation (EuCAP) (pp. 1-5). IEEE.
- [18] Huang, J., Cao, Y., Raimundo, X., Cheema, A., & Salous, S. (2019). Rain statistics investigation and rain attenuation modeling for millimeter-wave short-range fixed links. *IEEE Access*, 7, 156110-156120.
- [19] Popa, S., Draghiciu, N., & Reiz, R. (2008). Fading types in wireless communications systems. *Journal of Electrical and Electronics Engineering*, 1(1), 233-237.
- [20] Sun, S., MacCartney, G. R., & Rappaport, T. S. (2017, May). A novel millimeter-wave channel simulator and applications for 5G wireless communications. In 2017 IEEE International Conference on Communications (ICC) (pp. 1-7). IEEE

an Associate Professor of Electrical and Electronics Engineering at Ondokuz Mayıs University. His research interests include Electromagnetic Fields, Microwave Techniques, Telecommunications, and Digital Signal Processing.

BIOGRAPHIES



AHMET FURKAN KOLA received his B.Sc. degree in Electronic and Communication Engineering from Istanbul Technical University in 2019. He is an Ph.D. candidate in the Department of Electrical and Electronics Engineering at Ondokuz Mayıs University. He is currently working as a

Research Assistant in Electrical and Electronics Engineering the Samsun University. His current research interests include Telecommunications, Wireless Communication channels, and Digital Signal Processing.



ÇETİN KURNAZ received his B.Sc. degree in Electrical and Electronic Engineering from the Ondokuz Mayıs University in 1999. He received an M.Sc. degree in Electrical and Electronics Engineering from the Ondokuz Mayıs University in 2002. He received a Ph.D. in Electrical and Electronics Engineering from the

Ondokuz Mayıs University in 2009. He is currently working as